

Quantum noise in the Josephson charge qubit

O. Astafiev,^{1,*} Yu. A. Pashkin,^{1,†} Y. Nakamura,^{1,2} T. Yamamoto,^{1,2} and J. S. Tsai^{1,2}

¹The Institute of Physical and Chemical Research (RIKEN), Wako, Saitama 351-0198, Japan

²NEC Fundamental and Environmental Research Laboratories, Tsukuba, Ibaraki 305-8501, Japan

(Dated: October 24, 2018)

We study decoherence of the Josephson charge qubit by measuring energy relaxation and dephasing with help of the single-shot readout. We found that the dominant energy relaxation process is a spontaneous emission induced by quantum noise coupled to the charge degree of freedom. Spectral density of the noise at high frequencies is roughly proportional to the qubit excitation energy.

PACS numbers: 03.67.-a, 74.50.+r, 85.25.Cp

Artificial two-level systems attract interest of researchers because such systems are believed to be used as quantum bits (qubits) — basic elements for quantum computers. Recently much progress has been achieved in experiments on the Josephson qubits [1, 2, 3, 4, 5, 6, 7, 8]. All these experiments have shown that qubits are affected by decoherence which becomes a key issue of research.

Decoherence of small Josephson circuits has been studied in a number of theoretical papers (see for example, Ref. [9, 10]). Recently, decoherence of Josephson charge qubits has been investigated experimentally for some special cases. For instance, in charge echo experiments, dephasing of the Josephson charge qubit has been characterized under a bias condition far from the charge degeneracy point [11]. Also, relaxation rate of charge qubits off the degeneracy point has been measured [6, 12]. Dephasing and energy relaxation were studied in a qubit with the charging-to-Josephson-energy ratio about unity, for which charge noise may also be important [2, 13]. However, to understand the origin of the decoherence, a systematic study of the qubits is of great importance.

In this work, we measure and analyze the qubit energy relaxation rate in a wide range of parameters. In other words, we use the qubit as a spectrum analyzer to study the noise of the environment [14]. We found that the quantum noise is an asymmetric charge noise, which causes energy relaxation with approximately linear frequency dependence (f -noise). We also measure dephasing rate of the qubit and found that it is consistent with an assumption that it is caused by the $1/f$ noise.

The device schematically shown in Fig. 1(a) (identical to that described in Ref. [15]) consists of a qubit and a readout part. The qubit is a Cooper-pair box [1] (an island with area of $40 \times 800 \text{ nm}^2$) connected to a reservoir through a tunnel junction of SQUID geometry with Josephson energy E_J controlled by external magnetic field. The readout part contains a charge trap island and an electrometer — a single electron transistor (SET). The trap is connected to the box through a highly resistive tunnel junction. To measure the box charge state, the

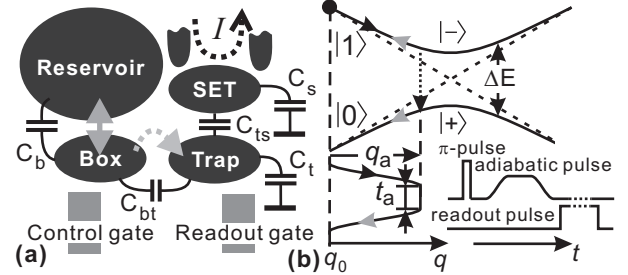


FIG. 1: (a) Schematic device representation. (b) State manipulation diagram for measurements of the qubit relaxation rate. The inset shows operation pulse sequence.

trap is biased by a readout pulse applied to the readout gate, so that if the box is in the excited state, an extra Cooper-pair charge tunnels into the trap in a sequential two-quasiparticle process and then detected by the SET. Note that the quantum states are not much decohered by the measurement circuit until the readout pulse is applied, as the SET is effectively decoupled from the qubit by serial capacitive dividers. Mutual and self capacitances of the islands are designated by C_{ij} and C_i , where i and j are characters b , t , and s , denoting the box, trap and SET islands, respectively. We have measured values of these capacitances ($C_b \approx 600 \text{ aF}$, $C_t \approx C_s \approx 1000 \text{ aF}$, $C_{bt} \approx 30 \text{ aF}$, $C_{st} \approx 100 \text{ aF}$) and also gate capacitances to their nearest islands. Other stray capacitances between the box and remote elements (between the box and each existing lead including the SET island and the ones not drawn in Fig. 1(a)) are calculated to be less than 0.3 aF . Electric field of those elements is strongly screened by the 100 nm thick Au ground plane beneath the 400 nm thick Si_3N_4 insulating layer. The box charging energy is $E_C \approx e^2/2C_b = 130 \text{ } \mu\text{eV}$ ($E_C/h = 32 \text{ GHz}$). The reservoir is a big island galvanically isolated from electrical leads and has capacitance of about 0.1 nF to the ground plane. The SET with $200\text{-k}\Omega$ junction resistances is usually biased at the Josephson quasiparticle cycle peak [16] with the maximum current of about 100 pA .

In the charge basis $|0\rangle$ and $|1\rangle$ (without and with an extra Cooper-pair in the box), the Hamiltonian of the

*Electronic address: astf@frl.cl.nec.co.jp

†On leave from Lebedev Physical Institute, Moscow 117924, Russia

box can be written as

$$H = -\frac{\Delta E}{2}[\sigma_z \cos \theta + \sigma_x \sin \theta], \quad (1)$$

where σ_z, σ_x are the Pauli matrices, $\Delta E = (U^2 + E_J^2)^{1/2}$, $U = 2eq/C_b$ is the electrostatic energy difference between the two states, q is a gate induced charge ($q \equiv 0$ at the degeneracy point) and $\theta = -\arctan(E_J/U)$. Eigenstates of the two-level system are $|+\rangle = \cos(\theta/2)|0\rangle + \sin(\theta/2)|1\rangle$ and $|-\rangle = -\sin(\theta/2)|0\rangle + \cos(\theta/2)|1\rangle$ with corresponding eigenenergies $-\Delta E/2$ and $\Delta E/2$. Fig. 1(b) schematically shows the energy diagram of the qubit as a function of q . Solid and dashed lines represent eigenenergies and electrostatic energies, respectively. We usually adjust the qubit to a position of q_0 (< 0), where $|U| \gg E_J$ and eigenstates are nearly pure charge states $|+\rangle \approx |0\rangle$ and $|-\rangle \approx |1\rangle$. For the coherent control of the qubit, we start from the ground state $|0\rangle$ and apply a rectangular pulse bringing the system nonadiabatically to the degeneracy point ($q = 0, \theta = \pi/2$) for the time t_p , where the state freely evolves as $\cos(E_J t/2\hbar)|0\rangle + i \sin(E_J t/2\hbar)|1\rangle$. We create state $|1\rangle$ by applying the pulse of length $t_p = 2\pi\hbar/E_J$ (π -pulse) [1].

To measure energy relaxation dynamics of the excited state $|-\rangle$ we use a combination of the π -pulse and an adiabatic pulse (a pulse with slow rise and fall times satisfying the condition of $\hbar|d\Delta E/dt| \ll E_J^2$). The manipulation procedure, schematically shown in Fig. 1(b), includes three sequential steps: First, the π -pulse is applied to the box to prepare the excited state $|1\rangle$. Second, an adiabatic pulse is applied to the box, so that its rise front shifts the system along the excited state $|-\rangle$ to a point $q = q_0 + q_a$ and holds the system at fixed q for a time t_a , where relaxation from the excited state $|-\rangle$ to the ground state $|+\rangle$ may occur with a finite probability dependent on t_a . Third, the fall of the adiabatic pulse converts the excited state $|-\rangle$ to the charge state $|1\rangle$ and the ground state $|+\rangle$ to state $|0\rangle$, respectively. One can study the relaxation dynamics at a desired value of q by measuring probability P of detecting the excited state $|1\rangle$ in the final state as a function of t_a .

We study two samples (I and II) of an identical geometry at a temperature of 50 mK. Probability P is determined by repeating nominally identical quantum state manipulations and readouts [15]. The inset of Fig. 2(a) exemplifies a typical decay of P as a function of t_a at $q = -0.36 e$ of sample I. We derive the energy relaxation rate Γ_1 by fitting the data with $A \exp(-\Gamma_1 t_a) + B$ using three fitting parameters A, B and Γ_1 . The amplitude A depends on the efficiency of each step of the state manipulations and is independent of t_a . A is a constant at fixed q , when all parameters except t_a are kept unchanged. A small finite value of B is a consequence of “dark” switches in our circuit. Note that in the present experiments B is always small independently of q , indicating that relaxation is much stronger than excitation.

Figs. 2 (a), (b) show Γ_1 as a function of q . Fig. 2(a) demonstrates Γ_1 (closed circles) measured in sample I

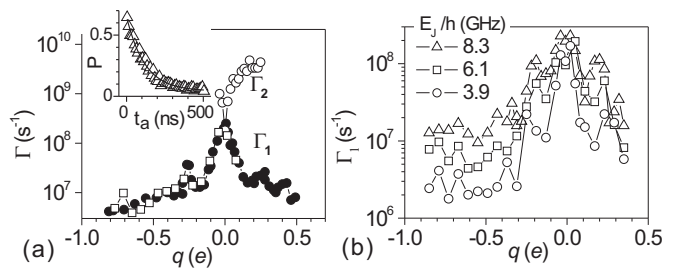


FIG. 2: (a) Energy relaxation rate Γ_1 measured by the SET normally set in the JQP peak (closed circles) and in blockade regime (open squares) and phase decoherence rate Γ_2 (open circles) versus gate induced charge q of sample I ($E_J/h = 5.1$ GHz). The inset exemplifies a decay of probability P to detect charge in the trap as a function of the adiabatic pulse length t_a , measured at $q = -0.36 e$. Γ_1 is derived from exponential fit of the decay. (b) Γ_1 measured in sample II for three different Josephson energies.

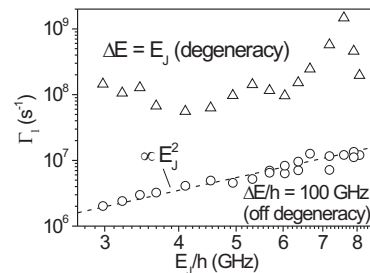


FIG. 3: Relaxation rate Γ_1 as a function of E_J measured at the degeneracy point (open triangles) and off the degeneracy point (open circles) at $\Delta E/h \approx 100$ GHz for sample I.

with $E_J/h = 5.1$ GHz. Fig. 2(b) shows Γ_1 in sample II measured for three different Josephson energies: $E_J/h = 3.9$ GHz (dots), 6.1 GHz (squares) and 8.3 GHz (triangles). E_J dependences of the relaxation rate Γ_1 for sample II at fixed adiabatic pulse amplitudes are shown in Fig. 3. Γ_1 at $q = -0.8 e$ ($\Delta E/h = 100$ GHz) is presented by open circles, while Γ_1 at $q = 0$ (degeneracy point) is presented by open triangles.

For the charge qubit, noises coupled to the qubit charge degree of freedom are presumably the main origin of decoherence. If the energy fluctuations of the qubit due to the charge noise are characterized by the spectral density of electrostatic energy fluctuations $S_U(\omega)$ [17], the relaxation rate is given by the Fermi’s golden rule (see e.g. Ref. [14])

$$\Gamma_1 = \frac{\pi S_U(\omega)}{2\hbar^2} \sin^2 \theta. \quad (2)$$

The overall behavior of Γ_1 in Figs. 2(a), (b) — Γ_1 decreases with increasing $|q|$ — is described by $\sin^2 \theta = E_J^2/(E_J^2 + U^2)$, characterizing coupling of the qubit to the reservoir via the charge degree of freedom. When $\Delta E \gg E_J$, Eq. (2) can be rewritten in the form $\Gamma_1 \approx \pi S_U(\omega \approx U/\hbar)(E_J/U)^2/(2\hbar^2)$. The experimen-

tally measured Γ_1 at $\Delta E/\hbar = 100$ GHz (open circles in Fig. 3) has clear E_J^2 -dependence (dashed curve). This confirms the dominant contribution of charge fluctuations. Moreover, it indicates that this relaxation process is Cooper-pair tunneling rather than sequential tunneling of two quasiparticles. At the degeneracy point, $\Gamma_1 = \pi S_U(\omega = E_J/\hbar)/2\hbar^2$ (open triangles in Fig. 3) directly reproduces frequency dependence of $S_U(\omega)$.

It is known that one of the main low-frequency noises in nano-scale charge devices is the $1/f$ noise produced by a bath of charge fluctuators. The spectral density of the charge fluctuations defined for negative and positive frequencies is given by

$$S_q(\omega) = \frac{\alpha}{2|\omega|}. \quad (3)$$

The parameter α has been found in a number of experiments to be typically of order of $(10^{-3}e)^2$ [11, 18, 19, 20]. It was also shown in charge echo experiments that the $1/f$ noise reasonably explains dephasing of the charge qubit [11].

Under an assumption of the Gaussian noise produced by many fluctuators weakly coupled to the qubit, the coherent oscillations dephase as $\exp[-\varphi(t)]$, as the random phase

$$\varphi(t) \approx \frac{\cos^2 \theta}{\hbar^2} \int_{\omega_0}^{\infty} S_U(\omega) \left[\frac{2 \sin(\omega t/2)}{\omega} \right]^2 d\omega \quad (4)$$

is accumulated from the low-frequency component of $S_U(\omega)$ ($|\omega| \leq 2\pi/t$), where $S_U(\omega) = (4E_C/e)^2 S_q(\omega)$. The phase decoherence time $T_2 = \Gamma_2^{-1}$ is defined as $\varphi(T_2) = 1$. From the experimentally observed decay of coherent oscillations, Γ_2 is obtained for various q in sample I (Fig. 2 (a)). Assuming the $1/f$ noise spectrum of Eq. (3), we obtain the parameter $\alpha = [\eta \hbar e \Gamma_2 / (E_c \cos \theta)]^2 \approx (1.3 \times 10^{-3}e)^2$, where η is a numeric coefficient weakly dependent on the lower cutoff frequency ω_0 [21].

Fig. 4(a) summarizes reduced noise spectra $S_U/\hbar^2 = 2\Gamma_1/(\pi \sin^2 \theta)$ derived from Γ_1 measurements. S_U/\hbar^2 derived from $\Gamma_1 - q$ dependences in sample I is plotted by closed circles, while S_U/\hbar^2 for sample II with different E_J is plotted by open circles. In addition, $S_U/\hbar^2 = 2\Gamma_1/\pi$ measured at the degeneracy point of sample II is plotted by open triangles. We also show S_U/\hbar^2 for the $1/f$ noise (Eq. (3)) with $\alpha = (1.3 \times 10^{-3}e)^2$ by the dashed line. The data exhibits rise with increasing ω . The dashed-dotted line exemplifies linear dependence (as in the case of ohmic environment), which we present in the form of $(4e^2/\pi)R\hbar\omega/\hbar^2$ with $R = 6 \Omega$. The actual rise of the experimental data is not monotonic but has some resonance-like peaks, for instance, at 7 and 30 GHz. This probably reflects coupling to some resonances, which can be other microscopic coherent two-level systems or geometrical resonances in the device. The crossover frequency of the $1/f$ and f curves is $\omega_c = 2\pi \times 2.6$ GHz, which formally corresponds to the temperature $T_c = \hbar\omega_c/k = 120$ mK.

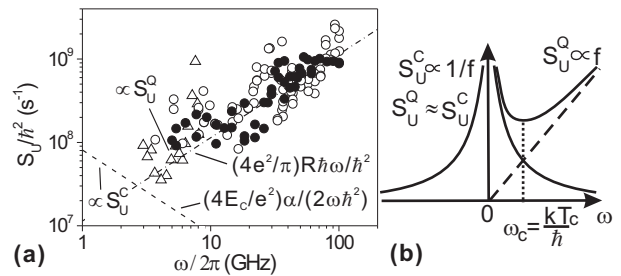


FIG. 4: (a) Noise S_U/\hbar^2 derived from $\Gamma_1 - q$ dependences of the sample I (closed circles) and sample II (open circles). Open triangles show Γ_1 dependences of sample II at the degeneracy point. A dashed-dotted line represents a linear rise $(4e^2/\pi)R\hbar\omega/\hbar^2$ (f noise) with $R = 6 \Omega$. A dashed line is the $1/f$ noise from Eq. (3) with $\alpha \approx (1.3 \times 10^{-3}e)^2$ derived from Γ_2 measurements. (b) A schematic representation of the classical $S_U^C(\omega)$ and quantum $S_U^Q(\omega)$ noise behavior. At frequencies $\omega < kT/\hbar$, $S_U^Q(\omega) \approx S_U^C(\omega)$ and behaves like a $1/f$ noise. At frequencies $|\omega| > kT/\hbar$, $S_U^Q(\omega) > S_U^C(\omega)$ and the quantum noise is proportional to ω .

We argue that in our device, the relaxation cannot be explained by coupling to electromagnetic environment through electrical leads of the gates and the readout circuit. The fact that the qubit relaxation is much stronger than excitation indicates that the relaxation is induced neither by radiation from hot environment nor by power dissipated in the measurement SET. For spontaneous emission to the environment, the lead impedance needed to explain Γ_1 is estimated. The control-gate-to-box capacitance $C_{cg} = 1$ aF gives coupling strength $\kappa_g = C_{cg}/C_b \approx 2 \times 10^{-3}$. Other leads have direct capacitances to the box smaller than 0.3 aF. Even for the indirect coupling to the box through the trap, the strongest coupling factor is $\kappa_g \approx C_{rg}C_{bt}/C_bC_t \approx 5 \times 10^{-3}$ to the readout gate (readout-gate-to-trap capacitance $C_{rg} \approx 10$ aF). The lead impedance required to explain Γ_1 is $R/\kappa_g^2 \sim 10^5 \Omega$ and much higher than the typical value of $\sim 100 \Omega$. Also, Γ_1 can not be explained by absorption on the SET. The box-to-SET coupling is $\kappa_s \approx C_{st}C_{bt}/C_bC_t \approx 5 \times 10^{-3}$ and SET impedance is substituted by $Z_s = R_s/(1 + i\omega C_s R_s)$, where $R_s \geq 100$ k Ω depends on the SET gate bias conditions with minimal value of two parallel tunnel junction resistances. The dissipative impedance for our qubit is $\kappa_s^2 \text{Re}[Z_s] \leq 1.6 \Omega$ at $\omega = 5$ GHz and rapidly decreases with frequency and resistance as $\omega^{-2}R_s^{-1}$. To check experimentally the effect of the SET noise, we compare in Fig. 2(a) Γ_1 obtained with SET biased at the JQP peak (closed circles) and in the blockade regime (open squares; SET current switches on only when charge is trapped). Independence of Γ_1 of bias conditions proves that the SET noise is not dominant in the qubit relaxation.

The observed E_J^2 -dependence shows that the dominant noise is coupled to the charge degree of freedom. However, with the discussions in the previous paragraph, we

exclude a possible contribution of the coupling to the electromagnetic environment through the leads. On the other hand, dephasing of our qubit is well explained by the $1/f$ noise produced by charge fluctuators. In standard models of the $1/f$ noise, the fluctuators are characterized by activation energy E^* and switching rate γ [22]. In thermal equilibrium, the charge fluctuators with excitation energies $E^* \leq kT$ are activated producing telegraph-like noise and contributing to the $1/f$ noise at frequency γ . However, we suppose that inactive fluctuators with $E^* \geq kT$ may absorb energy ΔE of our qubit, which is out of equilibrium with surrounding environment ($\Delta E > kT$). The thermally excited fluctuators produce the classical noise (without energy exchange with the qubit) S_U^C ($S_U^C(\omega) = S_U^C(-\omega)$) and cause the qubit dephasing, while the spontaneous emission is characterized by the quantum noise S_U^Q ($S_U^Q(|\omega|) > S_U^Q(-|\omega|)$). Namely, the “hot” qubit ($\Delta E > kT$) may only release the excess energy ΔE to the “cold” bath. Fig. 4(b) schematically represents the noise behavior extended to the negative frequency range. S_U^Q almost coincides with S_U^C at low frequencies $\hbar\omega \ll kT$ (“hot” bath), where the qubit has an equal chance to emit and to absorb energy. S_U^C is expected to have $1/f$ dependence, while S_U^Q at $\hbar\omega \gg kT$ (“cold” bath) is roughly proportional to f according to our experimental data.

The crossover frequency ω_c satisfies the condition

$\alpha/2\omega_c = \beta\hbar\omega_c$, where $\beta\hbar\omega$ is the f -noise characterized by temperature independent parameter β . The corresponding $1/f$ noise spectral density at $|\omega| \ll |\omega_c|$ is

$$S_U^C(\omega) = \frac{\beta(kT_c)^2}{\hbar|\omega|}. \quad (5)$$

This means that if T_c scales with surrounding temperature T , then the $1/f$ noise should have T^2 dependence. For instance, if the density of states of the fluctuators is constant or a weak function of two independent energies (for example, excitation energies of an electron in a double-well potential) then the $1/f$ noise is proportional to T^2 [23]. The temperature dependence of the $1/f$ -noise can be verified experimentally by measuring for example SET low frequency noise.

In conclusion, we have measured energy relaxation and dephasing of the Josephson charge qubit. The relaxation is a spontaneous emission process induced by the quantum charge noise nearly proportional to the qubit energy (f quantum noise). Dephasing of the qubit is explained by the $1/f$ noise. The f quantum noise crosses over the extrapolated $1/f$ classical noise (causing pure dephasing) at a frequency $\omega_c = kT_c/\hbar$, with $T_c \approx 120$ mK.

We thank B. Altshuler, D. Averin, P. Delsing, D. Esteve, G. Falci, S. Lloyd, E. Paladino, A. Shnirman and D. Vion for valuable discussions.

-
- [1] Y. Nakamura, Y. A. Pashkin, and J. S. Tsai, *Nature* **398**, 786 (1999).
- [2] D. Vion, A. Aassime, A. Cottet, P. Joyez, H. Pothier, C. Urbina, D. Esteve, and M. H. Devoret, *Science* **296**, 886 (2002).
- [3] Y. Yu, S. Han, X. Chu, S. I. Chu, and Z. Wang, *Science* **296**, 889 (2002).
- [4] J. M. Martinis, S. Nam, J. Aumentado, and C. Urbina, *Phys. Rev. Lett.* **89**, 117901 (2002).
- [5] I. Chiorescu, Y. Nakamura, C. J. P. M. Harmans, and J. E. Mooij, *Science* **299**, 1869 (2003).
- [6] T. Duty, D. Gunnarsson, K. Bladh, and P. Delsing, *Phys. Rev. B* **69**, 140503 (2004).
- [7] Y. A. Pashkin, T. Yamamoto, O. Astafiev, Y. Nakamura, D. V. Averin, and J. S. Tsai, *Nature* **421**, 823 (2003).
- [8] T. Yamamoto, Y. A. Pashkin, O. Astafiev, Y. Nakamura, and J. S. Tsai, *Nature* **425**, 941 (2003).
- [9] Y. Makhlin, G. Schön, and A. Shnirman, *Rev. Mod. Phys.* **73**, 357 (2001).
- [10] D. V. Averin, *Fortshr. Phys.* **48**, 1055 (2000).
- [11] Y. Nakamura, Y. A. Pashkin, T. Yamamoto, and J. S. Tsai, *Phys. Rev. Lett.* **88**, 047901 (2002).
- [12] K. W. Lehnert, K. Bladh, L. F. Spietz, D. Gunnarson, D. I. Schuster, P. Delsing, and R. J. Schoelkopf, *Phys. Rev. Lett.* **90**, 027002 (2003).
- [13] D. Vion, A. Aassime, A. Cottet, P. Joyez, H. Pothier, C. Urbina, D. Esteve, and M. Devoret, *Fortshr. Phys.* **51**, 462 (2003).
- [14] R. J. Schoelkopf, A. A. Clerk, S. M. Girvin, K. W. Lehnert, and M. Devoret, in *Quantum noise in mesoscopic physics.*, edited by Y. V. Nazarov (Kluwer, Dordrecht, 2002), pp. 175–203.
- [15] O. Astafiev, Y. A. Pashkin, T. Yamamoto, Y. Nakamura, and J. S. Tsai, *Phys. Rev. B* **69**, 180507 (2004).
- [16] T. A. Fulton, P. L. Gammel, D. J. Bishop, L. N. Dunkleberger, and G. J. Dolan, *Phys. Rev. Lett.* **63**, 1307 (1989).
- [17] Here, we define the spectral density for operator $\hat{g}(t)$ as $S_g(\omega) = \frac{1}{2\pi} \int_{-\infty}^{\infty} \langle \hat{g}(\tau)\hat{g}(0) \rangle e^{-i\omega\tau} d\tau$, where angular brackets represent quantum statistical averaging.
- [18] G. Zimmerli, T. M. Eiles, R. L. Kautz, and J. M. Martinis, *Appl. Phys. Lett.* **61**, 237 (1992).
- [19] S. M. Verbrugh, M. L. Benhamadi, E. H. Visscher, and J. E. Mooij, *J. Appl. Phys.* **78**, 2830 (1995).
- [20] H. Wolf, F. J. Ahlers, J. Niemeyer, H. Scherer, T. Weimann, A. B. Zorin, V. A. Krupenin, S. V. Lotkhov, and D. E. Presnov, *IEEE Trans. Instr. Meas.* **46**, 303 (1997).
- [21] Taking $\omega_0 = \pi/\tau_m$ with a typical measurement time of one data point $\tau_m = 0.6$ s, we find $\eta \approx 0.055$.
- [22] S. Kogan, *Electronic noise and fluctuators in solids* (Cambridge University Press, Cambridge, 1996).
- [23] M. Kenyon, C. J. Lobb, and F. C. Wellstood, *J. Appl. Phys.* **88**, 6536 (2000).